To appear: European Journal of Control, 2011.

A Motion Description Language for Robotic Reconnaissance of Unknown Fields

Dimitar Baronov and John Baillieul

Abstract

In this paper, we present two motion primitives that allow a mobile sensor to explore the features of an unknown scalar field. The first motion primitive is designed to follow and to map level contours (contours with constant value of the field). The second one steers the sensor to ascend or alternatively descend the field gradient and, as a result, to localize its extremum points. Both of these primitives are defined in terms of the geometric characteristics of the potential function and their performance is analyzed for different ranges of the parameters describing the geometry. The two motion primitives constitute a suitable library for rapid information acquisition aimed at the mapping of unknown fields. The motion control primitives developed bellow will provide the foundation of a theory of control for information acquisition in the exploration of unknown fields by means of mobile point sensors. This theory is treated in a companion paper.

I. Introduction

For many decades, there has been a notable level of interest in the relationship between control and other areas of information science and engineering. We refer to the compilations [1], [2], and [3] for accounts of some of the directions in which this research has evolved. Broadly speaking, information based control has historically been focused on the role of information in game and team theory strategies (see, e.g., [14], [21]), spatio-temporal patterns of information that occur in sensor localization, consensus, and multi-agent formation control (see the papers on graph

This work was supported by ODDR&E MURI10 Program Grant Number N00014-10-1-0952, by ODDR&E MURI07 Program Grant Number FA9550-07-1-0528, by the National Science Foundation ITR Program Grant Number DMI-0330171, all to Boston University.

D. Baronov and J. Baillieul are with the Department of Mechanical Engineering, Boston University, Boston, MA, 02215. {baronov,johnb}@bu.edu

theoretic methods in [1], [2], and [3]), and feedback control using data-rate limited feedback channels (for which we refer to [34], [29], [33], and [24]). The research presented bellow, in conjunction with a companion paper [13], presents results that are aimed at establishing a theory of *control for information acquisition*. More specifically, this paper introduces a small family of *mission specific* motion control primitives that are aimed at steering mobile point sensors using sensed environmental data while at the same time storing the data so as to construct maximally descriptive maps of the environment. The application of these control laws and the related reconnaissance strategies (as detailed in [13]) are aimed at efficient information acquisition regarding unknown scalar fields. While there is now a considerable literature regarding control of mobile sensors (which we briefly review below), the novelty of the control laws presented here and their use in the reconnaissance strategies of [13] is the explicit quantification of information and the notion of optimal climbing of *information gradients*.

The literature on exploration of unknown fields by mobile robotic sensors provides the context for the research described in this paper. (See, for instance, [10], [11], [36], [23], [18], [17], and [28].) A common theme in prior work is the exploration of unknown environments that are abstracted by scalar potential fields by using sensors with limited sensing range. The application of this type of search is almost universal, from environmental monitoring [23], where such quantities as species density, radioactivity, and so forth can only be measured at the position of the sensor, to the nano-scale imaging [9], where the main tool is the *Scanning Probe Microscope*, which acquires an image by scanning a point probe over a path on a sample. In general, algorithms that aim to efficiently acquire information about unknown potential fields can be called non-raster scan techniques—the main idea being that the raster scan, as the baseline solution to the problem, is also the most inefficient. Reference [5] provides a survey on several such approaches. We also note that the approach to exploration of unknown fields described in [13] offers a new perspective on the use of information metrics in *adaptive sensing* along the lines described in [31].

In this paper, we present control laws that allow a sensor carrying mechanism (vehicle, probe, etc.) to ascend (or equivalently descend) a potential surface, or to track level sets with a constant potential value. Such control laws enable a mobile sensor to map specific features of the potential field (isolines and extrema). A defining feature of these control laws is that they rely on the interaction between the moving sensor and sensed measurements of the unknown environment,

and therefore we designate them as *reactive motion primitives*. Part of the work in this paper has appeared in our previous papers [10] and [11]. Here, we extend this work to present a unified library of control laws that can provide the building blocks for complex strategies for monitoring and exploring potential fields, such as the ones presented in [8], [12], and a major companion paper [13].

We will distinguish between two different types of methods for designing *reactive search* motion primitives–methods that rely on a single sensor and methods that rely on an array of sensors. The second type is represented by the work in [36], [30], [37]. Reactive control algorithms for mobile sensor arrays are typically aimed at maintaining configurations that provide array data to estimate the field's geometric characteristics, e.g., gradient directions and curvature. The motion objectives are achieved by the agents being guided by two separate control laws–a shape control that keeps them in a rigid formation, and a reactive control, that allows them either to track a level set [36], [37], or move in the direction of the gradient [30].

The utilization of a single mobile platform equipped with a single sensor comes with the limitation of not being able to instantaneously estimate the gradient or any other higher-order characteristic of the potential surface. As is often the case, nature has found a way around this limitation. Through the process of chemotaxis, bacteria can navigate towards higher concentrations of oxygen, minerals or organic nutrients. E-coli, for instance, utilize a sensing-enabled protocol employing the alternation of two primitives–tumble in place and swim in straight line. If the bacterium perceives the concentration of food (L-Aspartate being a fovorite) as increasing, there is a higher probability to move forward, and if the potential is not changing, a higher probability to tumble in place [4]. In the robotic search realm, examples of strategies resembling or inspired by this behavior are [28], [19].

The control laws investigated in the current paper are within the single-mechanism-single-sensor framework. In comparison with the algorithms that use multiple moving sensors, we present a more parsimonious use of resources. An important feature of the work is a framework within which the performance of the control laws can be specified in terms of the geometric parameters of the potential surface. This framework requires the introduction of nonholonomic constraints in the kinematics of the mobile sensor carrier, a beneficial side effect that allows for easier real-life implementation. References [15], [16] also present control laws for reactive search with a nonholonomic vehicle, but the control laws there are time dependent. They apply

periodic perturbations to the steering rate, whereas the control laws discussed in this paper lead to smoother trajectories.

The contribution of the current work in comparison to our previous papers [10], [11] is an analysis of the control laws that establishes their applicability to a broader range of geometric parameters of the potential surface. Indeed, the implementation of the control laws explicitly involves curvature invariants of the unknown potential field. From this geometry, a precise understanding of the way the speed of the sensor carrying mechanism affects its performance can be achieved.

Although, this work deals with idealized sensor information, we note that the general setup, which treats unknown geometric parameters as perturbations, can easily incorporate sensor noise. We reserve this analysis for future work, and in this paper we focus on the fundamental principles that guide the design of feedback motion controls for exploring unknown potential fields.

We conclude this introduction with remarks about the broader research context into which the results of this paper fit and about the paper's title. Some time ago we became interested in the theoretical foundations of decision making in exploration and reconnaissance tasks. Within this large research domain, our focus has been on the reconnaissance of unknown scalar fields. In a companion paper [13], we have proposed strategies of exploration with sensor-equipped mobile robots that can be shown to efficiently acquire information about unknown scalar fields defined on planar domains. It is precisely the control laws described below that enable implementation of these strategies.

Finally, a word of explanation regarding the title is in order. It might seem strange that a mere two motion primitives should constitute the building blocks of a motion description language (MDL) in the sense that Manikonda *et al.* ([26]) write about MDL's. Nevertheless, it is shown in [13] that the set of complex motions that are realizable as alternating concatenations of our two motion primitives is rich enough to be used to completely specify a wide class of reconnaissance missions. Thus, while our motion description language uses only a two letter alphabet, it has sufficient *expressive power* to be useful in defining all motion strategies within a class that is of practical importance. This stands in sharp contrast to other problem settings in which it is challenging to determine whether a set of motion primitives can be used create all motion plans that are of interest. We refer to [26] for more information.

The paper is organized as follows. In the next section, we present the design framework for

the control laws, and in sections III and IV, we present respectively the control laws for isoline following and gradient ascending/descending.

II. Reactive potential field exploration

For what follows, we will assume that the mobile sensor motion is contained in a connected, and simply connected domain $X \subset \mathbb{R}^2$, further referred to as the *search domain*. The potential function, $f : X \to \mathbb{R}$, $\mathbf{r} \mapsto f(\mathbf{r})$, associated with the *search domain* abstracts the environment that the mobile sensor aims to explore. Naturally, we will impose mild regularity conditions on this function to prevent pathological behavior that would otherwise complicate the current discussion. To this end, we shall assume that this function is a Morse function within X. This implies that $f(\mathbf{r})$ has non-degenerate critical points, one consequence of which is that its critical points are isolated. (See [27] for a proof of this property.) Hence, there will be no areas for which the potential surface is flat, and therefore, we can rely on our control laws to be informed by the local changes of the potential field.

In the work that follows, a single sensor-equipped mechanism is evaluating a scalar function $f(\cdot)$ at a single point. Hence, the observations are given by $Y(t) = f(\mathbf{r}(t))$, which is the value of the scalar potential measured at the position of the mobile sensor, $\mathbf{r}(t) \in \mathbb{R}^2$. (The trajectory, $\mathbf{r}(t)$, is specified with respect to a fixed Cartesian coordinate frame.)

The general model for the resultant system is given by:

$$\dot{\mathbf{r}} = \mathbf{u}, \tag{1}$$

$$Y = f(\mathbf{r}(t)); \tag{2}$$

that is, the potential function can be thought of as a nonlinear observation function of sensed values along the trajectory of the mobile sensor. Note that at this point in the development, we are modeling the sensor carrying mechanism as a point with unconstrained motion in the plane.

A feedback control that maps the output, $Y(t)$, directly to a control input, $\mathbf{u}(t)$, will be called a *reactive control law*. Moving under such a control law, the sensor harvests information about the environment (the spatial distribution of $f(\mathbf{r})$) by controlling its trajectory solely based on the measurements it acquires. The underlying premise of the control designs below is that both the control objective and the control realization are expressed in terms of the sensor reading $Y(t)$. One example is keeping the output such that $Y(t)$ =const, while maintaining nonzero speed,

which makes the mobile sensor track a level set. Another example is steering the sensor such that $Y(t)$ is strictly increasing (or strictly decreasing), which leads to trajectories that ascend (or descend) the potential surface. The use of such primitives allows the mechanism to map local minima and maxima of the potential function. Inspired by the symbolic control literature, [26], we will further refer to such control laws as *motion primitives*, the idea being that a library of primitives can constitute a basis for search behaviors, as shown in [12].

A. *Modeling framework for describing sensor-environment interaction*

To formalize the objectives of the different motion primitives, one needs to define a framework in which the evolution of the measurements, $Y(t)$, is coupled explicitly to the motion of the sensor carrying mechanism. This can be addressed through dropping the Cartesian coordinate frame in favor of a nonlinear coordinate system defined by the geometry of the potential function.

The curvilinear coordinate system that we choose to work with has coordinate directions that are aligned with and transverse to the level sets of $f(\mathbf{r})$. The mild assumption of f being a harmonic function—i.e. that there is a harmonic conjugate $g : \mathbb{R}^2 \to \mathbb{R}$ satisfying:

$$\begin{aligned} \nabla g \cdot [1,\ 0]^T &= \nabla f \cdot [0,\ -1]^T \\ \nabla g \cdot [0,\ 1]^T &= \nabla f \cdot [1,\ 0]^T, \end{aligned}$$

where ∇ represents the gradient operator, guarantees that $\{f, g\}$ constitutes locally an orthogonal coordinate system. The utilization of such a setup will allow us to treat the functions $f(\mathbf{r})$ and $g(\mathbf{r})$ as local coordinate transformations from the Cartesian coordinate system, and thus, to analyze the trajectory of the sensor in terms of $[\tilde{f}(t), \tilde{g}(t)]$, where

$$\begin{aligned} \tilde{f}(t) &= f(\mathbf{r}(t)) \\ \tilde{g}(t) &= g(\mathbf{r}(t)). \end{aligned}$$

(Note that according to this definition and (2), it follows that $\tilde{f} = Y$, and therefore in what follows we will use them interchangeably.)

We note that the assumption of f being a harmonic function is not actually needed. Its main purpose is to define the curvilinear coordinates, $\{\tilde{f}, \tilde{g}\}$, as a local alternative to $\mathbf{r}$. However, in the convergence analysis of the control law only the $\tilde{f}$ coordinate will be used. Therefore, the

harmonic assumption can be viewed as nothing more than a convenient tool to illustrate the motion primitives objectives, and it does not affect their practical implementation.

Directly from (1), the equations of motion of the mobile sensor in the new coordinate frame yield:

$$\begin{aligned} \dot{\tilde{f}} &= \nabla f \cdot \dot{\mathbf{r}} = \nabla f \cdot \mathbf{u} \\ \dot{\tilde{g}} &= \nabla g \cdot \dot{\mathbf{r}} = \nabla g \cdot \mathbf{u}. \end{aligned} \tag{3}$$

We further show that in the new coordinate frame, $\{\tilde{f}, \tilde{g}\}$, the equations of motion explicitly involve such geometric invariants as curvature. Thus, the performance of a motion primitive can be defined in terms of intuitive, physical properties of the unknown potential surface.

We denote the magnitude of the gradient by:

$$M = \|\nabla f\|,$$

and the angle between the tangent to an isoline and the x axis of the Cartesian coordinate frame as α.

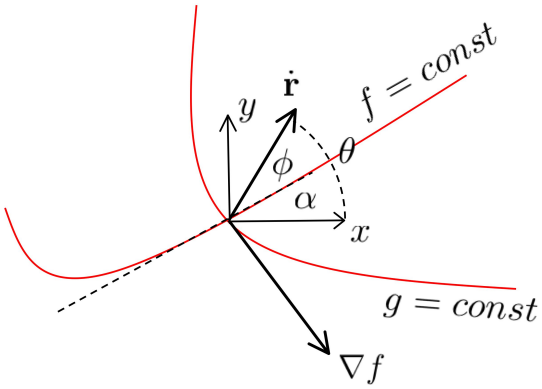

Fig. 1. The motion of the sensor in Cartesian and curvilinear coordinates. The depicted angles are as follows: θ corresponds to the heading of the vehicle relative to a fixed Cartesian coordinate frame; α corresponds to the angle between the tangent vector of a particular level set, $f = const$, at the position of the sensor and the x axis of the same coordinate frame; and $\phi = \theta - \alpha$ corresponds to the angle between the tangent vector and the velocity of the vehicle.

The notation is depicted in Fig. 1, where it should be noted that in terms of α and M,

$$\nabla f = M[\sin\alpha, -\cos\alpha]^T,$$

and

$$\nabla g = M[\cos\alpha, \sin\alpha]^T,$$

and hence equation (3) can be rewritten as

$$\begin{bmatrix} \dot{\tilde{f}} \\ \dot{\tilde{g}} \end{bmatrix} = M \begin{bmatrix} \sin\alpha & -\cos\alpha \\ \cos\alpha & \sin\alpha \end{bmatrix} \mathbf{u}. \tag{4}$$

On the other hand, on the trajectory of the sensor, α evolves according to

$$\begin{aligned} \dot{\alpha} &= \nabla\alpha \cdot \dot{\mathbf{r}} \\ &= \begin{bmatrix} (\frac{\partial \sin\alpha}{\partial x} - \frac{\partial \cos\alpha}{\partial y})\cos\alpha - (\frac{\partial \cos\alpha}{\partial x} + \frac{\partial \sin\alpha}{\partial y})\sin\alpha \\ (\frac{\partial \sin\alpha}{\partial x} - \frac{\partial \cos\alpha}{\partial y})\sin\alpha + (\frac{\partial \cos\alpha}{\partial x} + \frac{\partial \sin\alpha}{\partial y})\cos\alpha \end{bmatrix}^T \mathbf{u} \qquad (5) \\ &= \begin{bmatrix} \kappa_f \cos\alpha - \kappa_g \sin\alpha \\ \kappa_f \sin\alpha + \kappa_g \cos\alpha \end{bmatrix}^T \mathbf{u}, \qquad (6) \end{aligned}$$

where $\{x, y\}$ are the coordinates of the employed Cartesian system, and the divergence of the unit normal vectors to the isolines and the gradient lines are replaced with

$$\kappa_f = \nabla \cdot \left(\frac{\nabla f}{\|\nabla f\|} \right) \tag{7}$$

$$\kappa_g = \nabla \cdot \left(\frac{\nabla g}{\|\nabla g\|} \right), \tag{8}$$

which correspond to the curvatures of the contours $f(\mathbf{r}) = const$ and $g(\mathbf{r}) = const$ evaluated at the position of the sensor. (See [32] for information on level contours and their curvatures.)

The parameters κ_f and κ_g will have a closed form representation only for special potential functions. E.g., if the potential function is radial, there exists a choice of a point $\mathbf{r}_o$ and a function of a scalar variable $F : \mathbb{R} \to \mathbb{R}$ such that $f(\mathbf{r}) = F(\|\mathbf{r} - \mathbf{r}_o\|)$, for $\mathbf{r} \in X$. The two curvatures then satisfy:

$$\dot{\kappa}_f = \pm\kappa_f^2 \begin{bmatrix} \sin\alpha \\ -\cos\alpha \end{bmatrix}^T \mathbf{u} \tag{9}$$

and

$$\kappa_g = 0,$$

where the sign in (9) depends on the sign of $\frac{\partial F}{\partial r}$, $r = \|\mathbf{r} - \mathbf{r}_o\|$.

B. General control strategies

The system described by (4) and (5) has three unobservable parameters—the curvatures κ_f and κ_g, and the magnitude of the gradient, M. The estimation of these parameters, that are second and third order characteristics of the potential surface geometry, requires the sampling of the field at at least three non-collinear points. If the mobile entity relies on an array of sensors as in [36], [30], the control can explicitly implement such an observer. In the current set-up, however, an explicit estimation will require trajectories that allow the sensor carrying mechanism to utilize a single sensor in achieving this by sampling the field at enough points. Instead of relying on the estimation of these parameters, in what follows, we choose to treat them as unknown disturbances, so as to design strategies that can perform well given that the disturbances are bounded. We note that in neighborhoods of the critical points, such an assumptions will be invalid, which will become apparent in the analysis that follows.

In terms of the observation, $Y(t) = f(\mathbf{r}(t))$, the objectives of the different motion primitives can be specified as follows.

Isoline Following-given a fixed potential value, f_d, and non-zero speed, $\|\mathbf{u}\| > \epsilon > 0$, steer the sensor carrying mechanism such that

$$|Y(t) - f_d| = 0, \forall t > t^*, \tag{10}$$

which equivalently can be interpreted as the sensor mapping a connected level set.

Gradient Ascend/Descend- for a neighborhood $\Omega \subseteq X$, that does not contain critical points, achieve

$$\frac{dY(t)}{dt} = M\|\mathbf{u}\|, \forall \mathbf{r}(t) \in \Omega, \tag{11}$$

or alternatively

$$\frac{dY(t)}{dt} = -M\|\mathbf{u}\|, \forall \mathbf{r}(t) \in \Omega, \tag{12}$$

with non-zero speed, $\|\mathbf{u}\| > \epsilon > 0$, which will make the sensor follow the gradient and respectively either ascend or descend the potential surface.

We will further refer to these specifications as the idealized performance of the motion primitives. Because the variables κ_f, κ_g, and M are unknown, achieving such idealized performance will be challenging. Our approach will be to describe the system in terms of a nominal base and added perturbation terms. Given no perturbations, we would expect the control law to steer

the system such that it performs exactly according to the specifications, and given bounded perturbations, such that it achieves performance that is within a neighborhood around the ideal one.

We define the control $\mathbf{u}$ as:

$$\mathbf{u} = v[\cos\theta, \sin\theta]^T, \tag{13}$$

where θ is the angle of $\dot{\mathbf{r}}$ relative to the x axes of the Cartesian coordinate system, and v is the speed

$$v = \|\mathbf{u}\|.$$

Accordingly, we can also define the heading of the sensor carrying mechanism relative to the $\tilde{f}$ coordinate of the nonlinear coordinate system, $\{\tilde{f}, \tilde{g}\}$, as ϕ, where it can be observed in Fig. 1 that

$$\phi = \theta - \alpha.$$

Substituting (13) in (4) and (5) and exploiting some elementary trigonometric identities then yields:

$$\begin{bmatrix} \dot{\tilde{f}} \\ \dot{\phi} \end{bmatrix} = \begin{bmatrix} -vM\sin\phi \\ \dot{\theta} - v\kappa_f\cos\phi - v\kappa_g\sin\phi \end{bmatrix}. \tag{14}$$

This can be rewritten as

$$\begin{bmatrix} \dot{\tilde{f}} \\ \dot{\phi} \end{bmatrix} = \begin{bmatrix} -v\bar{M}\sin\phi \\ \dot{\theta} \end{bmatrix} + \begin{bmatrix} v\left(\bar{M} - M\right)\sin\phi \\ -v\kappa_f\cos\phi - v\kappa_g\sin\phi \end{bmatrix}.$$

Assuming that $\bar{M}$ is a known bound on the magnitude of the gradient within the area the sensor moves ($\bar{M} \leq M$), the first vector of this equation will correspond to the nominal system and the second vector to the perturbations. In terms of (14), isoline following, (10), will be equivalent to the system being stabilized to an equilibrium

$$\{\tilde{f} = f_d, \phi = 0\}; \tag{15}$$

that is the sensor carrying mechanism moves on the contour $f(\mathbf{r}) = f_d$. The descending/ascending control (respectively (11) and (12)), on the other hand, will correspond to the system converging to a manifold

$$\phi = \frac{\pi}{2} \tag{16}$$

or

$$\phi = 3\frac{\pi}{2}. \tag{17}$$

In the next two sections, equation (14) will be used to define two different control laws and to analyze their convergence properties. These control laws will accomplish the motion primitives specifications. This analysis will be performed with respect to different geometric parameters of the potential field, which will establish the applicability of these feedback routines in various scales and scenarios.

To conclude this section, we note that in the proposed control setup represented by (14), the control action appears as the steering rate $\dot{\theta}$ and the speed v. Going back to the Cartesian coordinate system, this translates to the sensor being driven by,

$$\begin{aligned} \dot{\mathbf{r}} &= v \begin{bmatrix} \cos\theta \\ \sin\theta \end{bmatrix} \\ \dot{\theta} &= \omega. \end{aligned} \tag{18}$$

In other words, in the pursuit of splitting the system into a nominal and a perturbed part, we have effectively introduced nonholonomic constraints. In what follows, we will treat the speed, v, as fixed, and hence, the feedback control law will be implemented via the steering, ω.

III. Isoline following

As discussed in the previous section, isoline following corresponds to stabilizing (14) to $\{\tilde{f} = f_d, \phi = 0\}$, with a finite non-zero speed, where f_d is the desired potential level to be followed. Thus, the sensor is controlled such that its position coincides with the chosen level set, while its velocity is tangent to it. Usually, in the generic scenario, a control law for contour following utilizes the curvature of the contour, e.g., [25], [20], [35]. In our set-up, however, the curvature is unknown (and treated as a disturbance), and therefore it is natural to expect that such exact following will be impossible. Instead, we will aim at steering and confining the sensor to a neighborhood:

$$\sqrt{(Y(t) - f_d)^2 + \phi^2} \leq c, \tag{19}$$

where $0 < c < \frac{\pi}{2}$ is an arbitrarily chosen constant, and $Y(t)$, as in (2), is the potential measured at the position of the sensor.

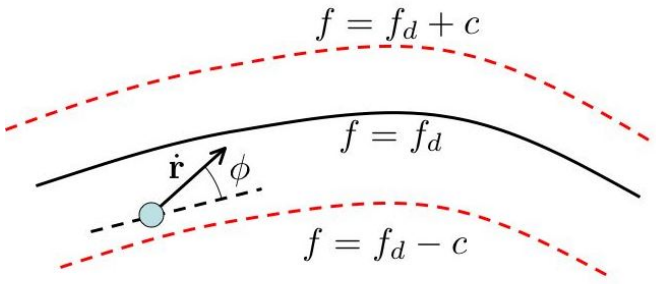

Fig. 2. Following an isoline within a neighborhood in curvilinear coordinates.

Fig. 2 illustrates the appearance of this neighborhood in Cartesian coordinates. The possible trajectories that yield (19) are restricted to a band around the desired isoline contour and since $|\phi| < \frac{\pi}{2}$ the associated velocities will be always pointing in a positive direction relative to the tangent vector of a neighboring level set, thus traversing the band along the desired contour.

Our aim is to show that given finite disturbances (M, κ_f, and κ_g), a constant speed, v, can be prescribed such that an appropriately defined feedback control maintains the motion of the sensor within an arbitrary small tubular neighborhood of the above form.

The control law that we propose to achieve this objective is

$$\omega = \frac{K_1}{v}(Y - f_d) + \frac{K_2}{v}\nabla f \cdot \dot{\mathbf{r}}, \tag{20}$$

where K_1, K_2, and v are constants that have to be chosen with respect to the geometry of the potential function.

The term $\nabla f \cdot \dot{\mathbf{r}}$ is the directional derivative of the potential field along the trajectory of the sensor, which in the curvilinear coordinates yields $\dot{\tilde{f}} = -vM \sin\phi$. In general, it can be estimated by a differentiation filter from the measurement, $Y(t)$. However, if this control law is applied directly to the heading, θ, we have

$$\begin{aligned} \theta(t) &= \int_0^t \omega(\tau)d\tau = \frac{K_1}{v}\int_0^t \left((Y(\tau) - f_d) + \frac{K_2}{v}\dot{\tilde{f}}(\tau)\right) d\tau \\ &= \frac{K_1}{v}\int_0^t (Y(\tau) - f_d)d\tau + \frac{K_2}{v}Y(t), \end{aligned} \tag{21}$$

and the estimation of the derivative is not needed. In the analysis that follows, we will find it convenient to use the form given by (20).

The next theorem shows a general stability result that will be further applied to establish that the proposed control law steers the system to a neighborhood of the form shown on Fig. 2.

Theorem 1: [22] Take the system $\dot{x} = h(x)$, and let $V(x)$ be a continuously differentiable function such that

$$c_1||x||^2 \leq V(x) \leq c_2||x||^2,$$

and

$$\frac{\partial V}{\partial x}h(x) < -W(x) \leq 0, \ \forall x \text{ s.t. } \beta \geq ||x|| \geq \nu > 0$$

where c_1, c_2, and β are positive constants, and $W(x)$ is a continuous positive definite function. Suppose that

$$\nu < \sqrt{\frac{c_1}{c_2}}\beta. \tag{22}$$

Then for every initial state $x(t_0)$ satisfying $\|x\| \leq \sqrt{\frac{c_1}{c_2}}\beta$, there is $T \geq 0$ such that the solution of the system $\dot{x} = h(x)$ satisfies

$$\|x(t)\| \leq \sqrt{\frac{c_2}{c_1}}\nu, \forall t \geq t_0 + T. \tag{23}$$

Applying this theorem to the system described by (14) and controlled by (20) yields the following result.

Theorem 2: Define $\dot{\theta} = \omega$, where ω is given by (20), for the system described by (14). Suppose that in an arbitrary connected neighborhood $\{\mathbf{r} : |f(\mathbf{r}) - f_d| < c\}$ the geometric parameters satisfy $M > \bar{M}$, $|\kappa_f| < \bar{\kappa}_f$, and $|\kappa_g| < \bar{\kappa}_g$, for some positive constants $\bar{M}$, $\bar{\kappa}_f$, and $\bar{\kappa}_g$. Then, given any c satisfying $0 < c < \frac{\pi}{2}$, there exists a choice of control parameters (K_1, K_2, and v) for which the system is contained within

$$\sqrt{(Y(t) - f_d)^2 + \phi(t)^2} \leq c.$$

Proof: We begin by introducing a change of variables, $x_1 = \frac{\tilde{f} - f_d}{v}$, $x_2 = \phi$. Transforming (14) accordingly yields:

$$\begin{aligned} \dot{x}_1 &= -M \sin x_2 \\ \dot{x}_2 &= K_1 x_1 - K_2 M \sin x_2 - v\kappa_f \cos x_2 - v\kappa_g \sin x_2. \end{aligned}$$

The candidate Lyapunov function is given by:

$$V(x_1, x_2) = x_1^2 - x_1 x_2 + 2(1 - \cos(x_2)).$$

It can be shown that in the interval $x_2 \in \left[-\frac{\pi}{2}, \frac{\pi}{2}\right]$ the following relationship holds

$$\frac{x_2^2}{2} \leq 2(1-\cos(x_2)) \leq x_2^2.$$

Therefore

$$V(x_1, x_2) \geq x_1^2 - x_1 x_2 + \frac{1}{2}x_2^2 \geq c_1\left(x_1^2 + x_2^2\right), \tag{24}$$

and

$$V(x_1, x_2) \leq x_1^2 - x_1 x_2 + x_2^2 \leq c_2\left(x_1^2 + x_2^2\right), \tag{25}$$

where

$$\begin{aligned} c_1 &= \frac{3-\sqrt{5}}{4} \\ c_2 &= \frac{3}{2}. \end{aligned}$$

The derivative of the Lyapunov function can be written as:

$$\dot{V}(x_1, x_2) = -\mathbf{x}^T P \mathbf{x} + vR\mathbf{x},$$

where $\mathbf{x} = \{x_1, x_2\}$, and P and R are respectively defined as:

$$P = \begin{bmatrix} K_1 & -\frac{\sin x_2}{x_2}\left(M\left(\frac{1}{2}K_2 - 1\right) + K_1\right) \\ -\frac{\sin x_2}{x_2}\left(M\left(\frac{1}{2}K_2 - 1\right) + K_1\right) & M\left(2K_2 - \frac{x_2}{\sin x_2}\right)\left(\frac{\sin x_2}{x_2}\right)^2 \end{bmatrix},$$

and

$$R = (\kappa_f \cos x_2 + \kappa_g \sin x_2)\begin{bmatrix} 1 & -2\frac{\sin x_2}{x_2} \end{bmatrix}.$$

It is important to note that:

$$\lim_{x_2 \to 0} \frac{x_2}{\sin x_2} = 1,$$

and $\frac{x_2}{\sin x_2} \in [1, \frac{\pi}{2}]$ for $x_2 \in \left[-\frac{\pi}{2}, \frac{\pi}{2}\right]$. Therefore, by arbitrarily choosing $K_2 = 2$, P can be made positive definite by choosing K_1 such that

$$K_1 < \bar{M}\left(4 - \frac{\pi}{2}\right) < M\left(4 - \frac{x_2}{\sin x_2}\right),$$

where $\bar{M} \leq M$.

Once P is made positive definite, taking into account that

$$0 < \frac{\sin x_2}{x_2} \leq 1, \; x_2 \in \left[-\frac{\pi}{2}, \frac{\pi}{2}\right],$$

the derivative of the Lyapunov function yields

$$\dot{V}(x_1, x_2) \leq -\lambda_{min}(P)\|x\|^2 + v\sqrt{3\left(\kappa_f^2 + \kappa_g^2\right)}\|x\|, \;\; \|x\| \leq \frac{\pi}{2}$$

where $\lambda_{min}(P)$ is the minimum eigenvalue of P for $x_2 \in \left[-\frac{\pi}{2}, \frac{\pi}{2}\right]$.

We define b as:

$$b = \sqrt{\frac{\sqrt{3\left(\kappa_f^2 + \kappa_g^2\right)}}{\lambda_{min}(P)}},$$

and as long as $\sqrt{v}b < \frac{\pi}{2}$, it follows that $\dot{V} < 0$ for all $\|x\|$ in the set $\sqrt{v}b \leq \|x\| \leq \frac{\pi}{2}$. According to Thm. 1, this will imply that the system is contained within the ball:

$$\|x\| \leq \sqrt{\frac{c_2}{c_1}}\sqrt{v}b,$$

where in addition

$$\min\left[\frac{1}{v}, 1\right]\sqrt{(Y - f_d)^2 + \phi^2} \leq \|x\|.$$

Therefore,

$$\sqrt{(Y - f_d)^2 + \phi^2} \leq \max[v, 1]\sqrt{\frac{c_2}{c_1}}\sqrt{v}b,$$

which implies that by appropriately choosing v, we can contain the system within any neighborhood chosen according to (19). ■

The effects of the potential function's geometry on the performance of the control law can be better understood through dividing the geometric parameters into two categories, *vanishing* and *non-vanishing* perturbations. The vanishing perturbations are the ones that vanish at the targeted manifold $\{f = f_d, \phi = 0\}$, and in (14) they are represented by $\bar{M} - M$ and κ_g, since they do not affect the system at $\phi = 0$. The non-vanishing perturbation is the curvature of the isoline, κ_f, since the term $v\kappa_f \cos\phi$ affects the system even when its trajectory evolves on the targeted manifold. The next corollary establishes that $\kappa_f \neq 0$ introduces a steady-state bias to the tracking of the isoline contour.

Corollary 1: Let the scalar potential function $f : X \to \mathbb{R}$ be a radial function, i.e. there exist a function $F(\|\mathbf{r}\|)$ such that $f(\mathbf{r}) = F(\|\mathbf{r}\|)$, and let the control law be given by (20). Then, for every choice of speed $v > 0$, there is a choice of control gains, K_1 and K_2, such that there exists a neighborhood of initial conditions for which the system satisfies

$$\begin{aligned} \lim_{t\to\infty}\left(\frac{K_1}{v}(Y(t) - f_d) - v\kappa_f\right) &= 0 \\ \lim_{t\to\infty}\phi(t) &= 0. \end{aligned}$$

Proof: We first assume an appropriately chosen origin of the Cartesian coordinate frame such that the potential function can be represented in terms of a function of a scalar variable, $f(\mathbf{r}) = F(r)$, where $r = \|\mathbf{r}\|$. It follows that the equilibrium that has to be proven stable satisfies

$$\frac{K_1}{v}(F(r) - f_d) - v\kappa_f = 0. \tag{26}$$

or in other words the systems should converge to a level set which is a solution of the equation:

$$F(r) = f_d + v^2 \frac{\kappa_f}{K_1}.$$

Here we will let $\mathbf{r}^*$ be a point such that $r^* = \|\mathbf{r}^*\|$ solves (26).

Note here that it can be shown that if $F'(r) > 0$, $\kappa_f = \frac{1}{r}$ and $\kappa_f = -\frac{1}{r}$ otherwise. Therefore, the term $v^2 \frac{\kappa_f}{K_1}$ acts to reduce the curvature of the level set that the sensor follows, and moreover r^* is a unique solution of (26). These observations motivate the following candidate Lyapunov function

$$V(\tilde{f}, \phi) = \int_{f(\mathbf{r}^*)}^{\tilde{f}} \frac{1}{vM} \left(\frac{K_1}{v}(y - f_d) - v\kappa_f \right) dy + (1 - \cos(\phi)).$$

Since r^* is unique, this function is a positive definite function for $\phi = \left[-\frac{\pi}{2}, \frac{\pi}{2}\right]$. Therefore, the convergence properties proved as a result of applying this candidate Lyapunov function will hold for a neighborhood $V(\tilde{f}, \phi) \leq 1$.

From the fact that f is radial, it follows that both M and κ_f can be represented solely as functions of the potential value at the position of the sensor. Therefore the derivative yields

$$\dot{V}(\tilde{f}, \phi) = -K_2 M \sin^2 \phi + v\kappa_f (1 - \cos \phi) \sin \phi \leq -(K_2 M - v |\kappa_f|) \sin^2 \phi,$$

and by choosing:

$$K_2 \geq \frac{v|\kappa_f|}{M},$$

we can guarantee that $\dot{V} \leq 0$. The LaSalle invariance principal [22], on the other hand, establishes that under this condition the equilibrium point is asymptotically stable. ■

A Simulated Example: We do not yet have a complete understanding of feedback designs for optimal performance of control laws of the form (20). Experience with both simulations and laboratory implementations indicates that there are wide ranges of gain parameters K_1 and K_2 such that the control law (20) steers the vehicle rapidly into a small neighborhood surrounding the desired isoline. In order to illustrate the above discussion regarding steady-state bias and the interpretation of high curvature as a disturbance, we have deliberately sought gain parameters

that are mistuned so as to cause noticeable deviations from the prescribed isoline path. Thus, Fig. 3 illustrates the effect of the curvature on the tracking error. It can be clearly observed how $Y(t) - f_d$ changes sign as the curvature changes from negative to positive.

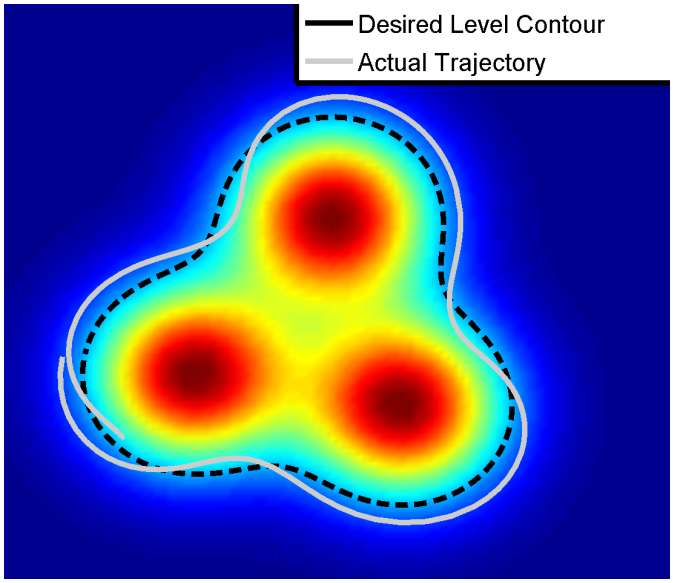

Fig. 3. An example of applying the control law given by (20) for following an isoline contour that has varying curvature sign.

IV. Descend/Ascend

Without loss of generality, in this section we will consider only an ascending motion primitive. The case of a descending motion primitive has a completely analogous treatment.

An optimal ascend control should guide the sensor such that it follows the gradient—the steepest path on the potential surface. In this case, the ascend rate is

$$\nabla f \cdot \dot{\mathbf{r}} = vM,$$

but since we do not have explicit knowledge of the gradient vector, our goal will be to steer the sensor carrying mechanism such that it ascends the potential surface with rate that exceeds a lower bound. As in the isoline following control law, this performance will be conditioned on the geometric parameters (treated as disturbances) being bounded. However, since an ascending path will lead to a local extremum, there is some neighborhood of the critical point at which the perturbations will fail to satisfy the assumption. Hence, we pursue a control law that can steer

the sensor carrying mechanism to a bounded ascend rate in finite time, and maintain this rate as long as the perturbations are within the assumed bounds. As a result, it will be shown that the sensor will ascend the potential surface until it reaches a neighborhood of a critical point.

The proposed control law to accomplish this task is

$$\omega = K_1(1 - K_2 \nabla f \cdot \dot{\mathbf{r}}). \tag{27}$$

As in the previous section, $\nabla f \cdot \dot{\mathbf{r}}$ can be either numerically estimated from the measurements, $Y(t) = f(\mathbf{r}(t))$, or the control law can be directly applied to the heading of the sensor, θ. (See (21).) Again, we will find it advantageous to analyze the control law from the perspective that it steers the sensor through $\omega = \dot{\theta}$.

The next theorem establishes that (27) will guide the sensor such that it reaches and maintains the desired ascend rate. The implications of this theorem in terms of geometric features of the potential surface are presented as separate corollaries.

Theorem 3: Let a connected set $\Omega \subseteq X$ satisfy:

$$M > \bar{M}, |\kappa_f| \leq \bar{\kappa_f}, |\kappa_g| \leq \bar{\kappa}_g, \forall \mathbf{r} \in \Omega,$$

for some positive constants $\bar{M}, \bar{\kappa}_f$, and $\bar{\kappa}_g$. (Note that $M > \bar{M} > 0$ implies that there are no local extremum points (min, max) in Ω.) Suppose that under the control (27) the system described in $\{\tilde{f}, \phi\}$ space by (14), and in Cartesian coordinates by (18) is initialized with $\mathbf{r}(0) = \mathbf{r}_0$ and $\phi(0) = \phi_0$ such that

$$\phi_0 \notin \left(\frac{3\pi}{2}, 2\pi\right),$$

and such that the ball $B_\delta = \{\mathbf{r} \in \mathbb{R}^2 : \|\mathbf{r} - \mathbf{r}_0\| < \delta\}$ satisfies

$$B_\delta \subset \Omega,$$

for some arbitrarily small δ.

Then, there is a choice of gains, K_1 and K_2, for which there exists a time $T \geq 0$ such that

$$\mathbf{r}(t) \in B_\delta \ \forall t \in [0, T],$$

and

$$\nabla f|_{\mathbf{r}(t)} \cdot \dot{\mathbf{r}}(t) \geq \beta v \bar{M}, \ \forall t \geq T \text{ provided } \mathbf{r}(t) \in \Omega, \tag{28}$$

where $0 < \beta < 1$ is an arbitrary constant.

Proof: From (14), $\nabla f \cdot \dot{\mathbf{r}}$ satisfying (28) yields:

$$\beta \bar{M} \leq -M \sin\phi,$$

which is equivalent to:

$$\sin^{-1}\frac{\beta\bar{M}}{M} + \pi \leq \phi \leq 2\pi - \sin^{-1}\frac{\beta\bar{M}}{M},$$

which we will equivalently denote as:

$$\phi_a^* \leq \phi \leq \phi_b^*.$$

Fig. 4 depicts the domain where the bounded ascent rate is satisfied in the $\{\tilde{f}, \phi\}$ phase plane. The rest of the proof will focus on showing that the trajectory reaches this domain in finite time, and stays there as long as the theorem conditions are satisfied. Specifically, we will choose

$$K_2 = \frac{1}{v\bar{M}}\left(1 + \frac{v\bar{\kappa}_g}{K_1}\right), \tag{29}$$

and will show that there exist values for the gain K_1 such that ϕ is contained within a trapping region, $\left[\phi_a^*, \frac{3\pi}{2}\right]$ and such that this this trapping region is attracting for all $\phi \in [0, \phi_a^*]$. (See Fig. 4 for an illustration of this conjecture in terms of the general directions of the vector field in the $\{\tilde{f}, \phi\}$ phase plane.)

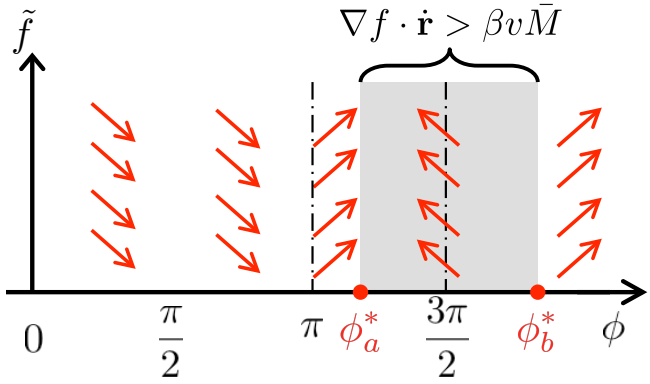

Fig. 4. The sign of $\dot{\phi}$ as function of ϕ. The changes of sign occur at points $\phi_1 \in \left[\phi_a^*, \frac{3\pi}{2}\right]$ and $\phi_2 \in \left[\frac{3\pi}{2}, 0\right]$, which are not depicted in the figure.

Substituting $\phi = \frac{3\pi}{2}$ and K_2 from (29) in the second equation of (14) yields

$$\dot{\phi} = K_1\left(1 - \frac{M}{\bar{M}}\right) - v\bar{\kappa}_g + v\kappa_g < 0.$$

On the other hand, setting $\phi = \phi_a^*$ yields

$$\begin{aligned}\dot{\phi} &= K_1(1-\beta) - v\beta\bar{\kappa}_g - v\kappa_f \cos\frac{\beta\bar{M}}{M} - v\kappa_g \sin\frac{\beta\bar{M}}{M} \\ &> K_1(1-\beta) - v\left(\beta\bar{\kappa}_g + \sqrt{\bar{\kappa}_g^2 + \bar{\kappa}_f^2}\right),\end{aligned}$$

an inequality which also holds for $\phi \in [0, \phi_a^*]$. Since $\beta < 1$, K_1 can be chosen large enough to make this expression satisfy $\dot{\phi} > 0$. In this case, starting from any initial position $\phi_0 \in [0, \phi_a^*]$, a bound on the time for which the sensor will reach the trapping region (and start climbing with a bounded rate) is given by:

$$\begin{aligned}T &< |\phi^* - \phi_0| \Big/ \inf_{\phi\in[-2\pi,\phi^*]}\left[\dot{\phi}\right] \\ &< \frac{\phi^* - \phi_0}{K_1(1-\beta) - v\left(\beta\bar{\kappa}_g + \sqrt{\bar{\kappa}_g^2 + \bar{\kappa}_f^2}\right)}.\end{aligned}$$

Since $T \to 0$ as $K_1 \to \infty$, the gain K_1 provides a control over the time that it takes the sensor to converge to the desired bounded ascend rate. On the other hand, if ϕ_0 is in the trapping region, the bounded ascend rate will be achieved for $T = 0$. (See Fig. 4 for an illustration of this proof.)

■

This theorem establishes that if the geometric parameters are bounded, the sensor can achieve a bounded ascend rate in an arbitrarily small neighborhood from its starting position, and stably maintain this rate as long as this condition is satisfied. To further establish the implication of this behavior, we will consider the trajectories that evolve in simply connected domains of the type $X = \{\mathbf{r} \in \mathbb{R}^2 : f(\mathbf{r}) \geq a\}$ that contain only a single local maximum, $\mathbf{r}^*$. The fact that f is a Morse function will imply that the only singularity of the field is at $\mathbf{r}^*$ and that, excluding an arbitrary small neighborhood around this extremum point, one can always find a subset of the search domain that has well behaved geometric parameters.

Corollary 2: Let a Morse function $f : X \to [a, b] \subset \mathbb{R}$ satisfy $f|_{\partial X} = a$, where ∂X is the boundary of the search domain. (That is, we assume that the boundary ∂X is a level set of f.) Assume that $f(\mathbf{r})$ has a single extremum point within the search domain, $f(\mathbf{r}^*) = b$. Then, for all choices of constants c, d such that $a < c < d < b$, we can find gains K_1 and K_2 for the control law given by (27) such that for initial conditions:

$$\mathbf{r}_0 \in \{\mathbf{r} \in X : c \leq f(\mathbf{r}) \leq d\},$$

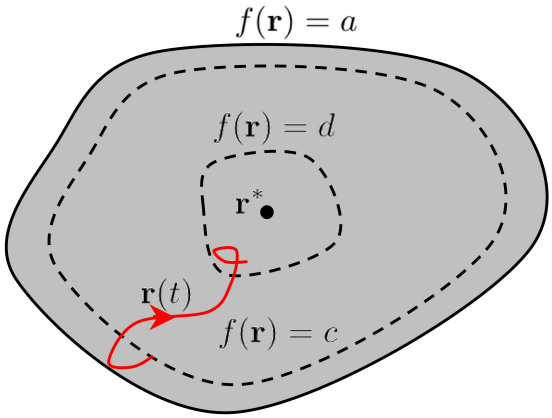

Fig. 5. An example trajectory illustrating the proof of Corollary 2

the system satisfies

$$\mathbf{r}(t) \in X, \forall t > 0$$

with associated time T,

$$f(\mathbf{r}(t)) \geq d, \ \forall t > T.$$

Proof: First, choose a positive constant δ such that $a \leq c - \delta$ and $b > d + \delta$. Since the only singularity is at $f(\mathbf{r}^*) = b$, we can find positive constants $\bar{\kappa}_f$, $\bar{\kappa}_g$, and $\bar{M}$ such that

$$\begin{aligned} \bar{\kappa}_f &\geq \sup_{\mathbf{r} \in D} |\kappa_f| \\ \bar{\kappa}_g &\geq \sup_{\mathbf{r} \in D} |\kappa_g| \\ \bar{M} &< \inf_{\mathbf{r} \in D} M, \end{aligned}$$

where D is the annulus

$$D = \{\mathbf{r} \in X : c - \delta \leq f(\mathbf{r}) \leq d + \delta\}.$$

From Theorem 3, by choosing K_2 according to (29), we can guarantee that under sufficiently large K_1 the system will be a) climbing with a rate that is bounded from bellow in D; and b) it cannot descend more than δ units before starting to ascend again. This proof is illustrated in Fig. 5. ■

We proceed to illustrate the properties of the control law by imposing additional assumptions on the potential function. We further show that under curtain geometries of the potential surface, the trajectory of the sensor carrying mechanism can be shown to converge to a limit cycle around the extremum point.

Corollary 3: Let $f(\mathbf{r})$ be a radial function, i.e. $f(\mathbf{r}) = F(\|\mathbf{r}-\mathbf{r}^*\|)$, where $\mathbf{r}^*$ is the coordinate of the maximum, and choose the gain K_2 of (27) to be

$$K_2 = \frac{1}{v\bar{M}}. \tag{30}$$

Then, if $M \geq \bar{M}$ for all $\mathbf{r}$ such that $\|\mathbf{r} - \mathbf{r}^*\| \geq \frac{v}{K_1}$, the trajectory of the system satisfies:

$$\lim_{t\to\infty} \|\mathbf{r}(t) - \mathbf{r}^*\| \to \frac{v}{K_1} \tag{31}$$

$\forall \mathbf{r}_0$ such that $\|\mathbf{r}_0 - \mathbf{r}^*\| > \frac{v}{K_1}$, and $\forall \phi_0$.

Proof: The proof proceeds as follows: first, we use a change of coordinates ($\tilde{f} \to r$), where $r = \|\mathbf{r} - \mathbf{r}^*\|$; then, we establish a trapping region for the trajectory as in the previous theorem; and finally, we use a Lyapunov function defined for a subset of the trapping region to show that the trajectory converges to the implied equilibrium point.

The parameter κ_f corresponds to curvature, and given the particular radial potential function, i.e. $F'(r) < 0$, it yields

$$\kappa_f = -\frac{1}{r}.$$

Therefore,

$$\begin{aligned} \dot{r} &= \sin\phi \\ \dot{\phi} &= K_1\left(1 + \frac{M}{\bar{M}}\sin\phi\right) + \frac{1}{r}\cos\phi, \end{aligned} \tag{32}$$

where without loss of generality, we have set $v = 1$, and also set $K_2 = \frac{1}{\bar{M}}$ in the control law of (27).

Equation (31) implies that the trajectory of (32) should converge to $r = \frac{1}{K_1}$, and it can be verified that $\{r = \frac{1}{K_1}, \phi = \pi\}$ is a fixed point for (32).

Now consider Fig. 6, and more specifically the lines denoted by 1 and 3, which correspond respectively to $\phi = \pi$ and $\phi = \frac{3\pi}{2}$ for $r \geq \frac{1}{K_1}$. On these lines, it can be easily verified that respectively $\dot{\phi} > 0$ and $\dot{\phi} < 0$. Therefore, the segment $\phi \in \left[\pi, \frac{3\pi}{2}\right]$, $r \geq \frac{1}{K_1}$, can be viewed as

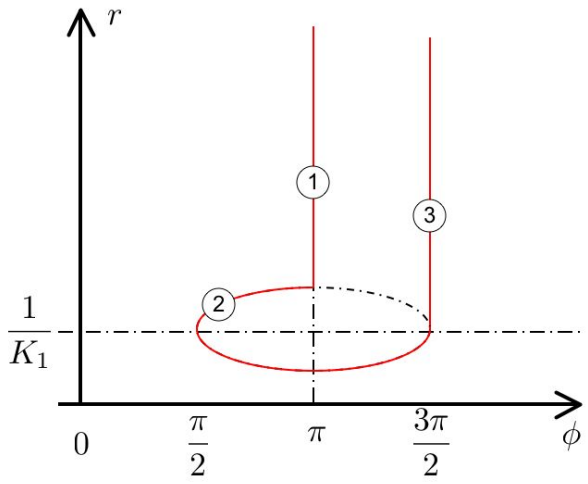

Fig. 6. A trapping region for the system given by (32). The first boundary is a segment on the line $\phi = \pi$, the second is a level set, $V(r, \phi) = 1$, of the function from (33), and the third is a segment of the line $\phi = \frac{3\pi}{2}$.

an attracting trapping region, which, since $\dot{r} < 0$, the trajectory can leave only through the line $r = \frac{1}{K_1}$. Now consider the boundary denoted by 2 in Fig. 6 as

$$V(r, \phi) = 1,$$

where $V(r, \phi)$ is a positive definite function for $\phi \in \left[\frac{\pi}{2}, \frac{3\pi}{2}\right]$ given by:

$$V(r, \phi) = \frac{1}{2}(rK_1 - 1)^2 + r(1 + \cos\phi), \tag{33}$$

with $V\left(\frac{1}{K_1}, \pi\right) = 0$. We have shown that once $\phi \in \left[\pi, \frac{3\pi}{2}\right]$, $r \geq \frac{1}{K_1}$, the trajectory will reach the interior $V(r, \phi) \leq 1$. Taking, the derivative of $V(r, \phi)$ on the trajectory of (32) yields

$$\dot{V}(r, \phi) = -rK_1 \frac{M}{\bar{M}} \sin^2\phi < 0.$$

The LaSalle invariance principle then implies that once in the interior of $V(r, \phi) \leq 1$, the trajectory converges to the desired equilibrium. ■

Fig. 7(a) illustrates the resultant trajectory of the sensor in the $\{r, \phi\}$ coordinate frame given that the gain K_2 satisfies (30). The trajectory converges to the point $(r, \phi) = \left(\frac{1}{K_1}, \pi\right)$. Fig. 7(b), on the other hand, shows the same trajectory in Cartesian coordinate frame.

A closer look at the proofs of the last two corollaries allows us to conclude the following qualitative relations associated with the control gains, K_1 and K_2. The gain K_1 determines the

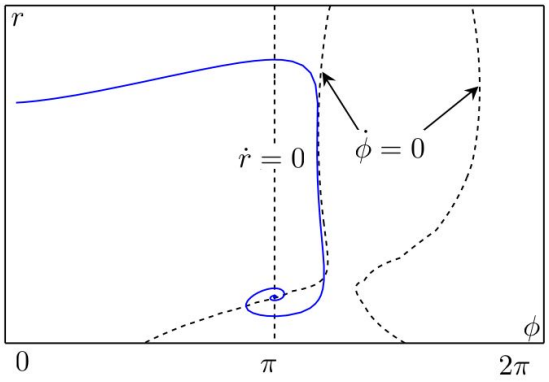

(a) A trajectory of the sensor carrying mechanism under the ascending control law in $\{\phi, r\}$ space,

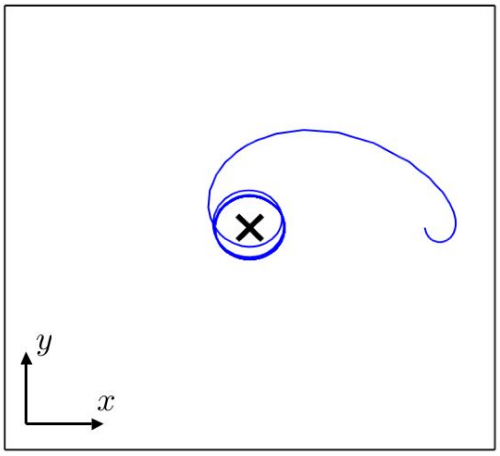

(b) and in the original, Cartesian coordinate system.

Fig. 7. Phase plot of the control law from Corollary 3 in Cartesian and in $\{\phi, r\}$ coordinates.

total turning rate at zero gradient ($M = 0$) and as such should be chosen according to the curvatures of the isolines and the gradient lines. The higher are the curvatures the faster turning rate is needed to suppress the perturbations that they cause. This can be clearly verified by Corollary 3, where the gain K_1 determines how close to the extremum point the mobile sensor can converge, and respectively what is the maximum isoline curvature that the control law can handle. The gain K_2, on the other hand, depends on the minimum magnitude of the gradient. It can be thought of as an amplification gain of the input signal, the input signal being the change of the potential on the trajectory of the sensor. Therefore, the flatter the potential field is, the

higher the gain K_2 should be.

From a control design perspective, the gain K_1 will be assigned depending on the minimum turning radius of the mobile sensor, and on the desired terminal proximity between the sensor and the extremum point. The choice of a value for the gain K_2, on the other hand, will be driven by the minimum value of the gradient of the field, and therefore will require some knowledge of the underlying phenomenon.

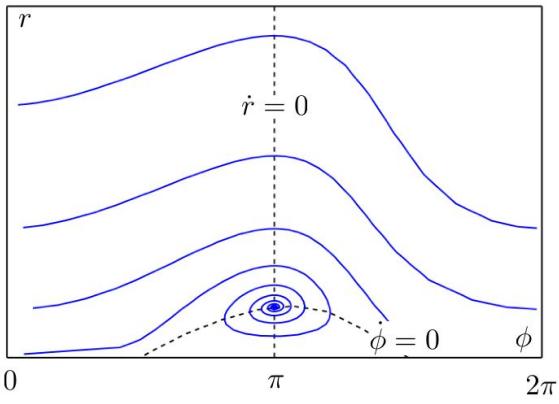

(a) A trajectory of the sensor carrying mechanism under the ascending control law in $\{\phi, r\}$ space,

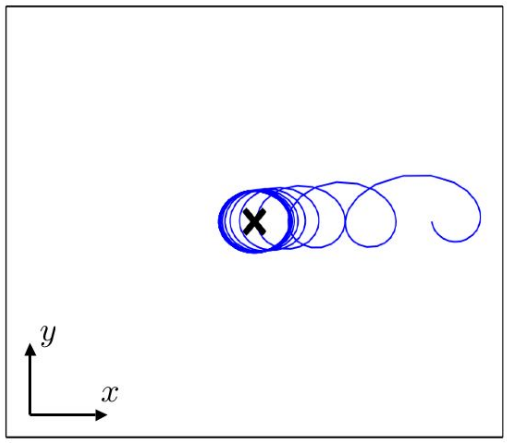

(b) and in the original, Cartesian, coordinate system.

Fig. 8. Phase plot of the ascending control law with a small gain K_2 in Cartesian and in $\{\phi, r\}$ coordinates.

Fig. 8 illustrates qualitatively the behavior of the mobile sensor, in the case that the gain K_2 is small, and therefore the control cannot assure a uniform (stable) ascent. The trajectory of the

sensor is shown in both cartesian coordinates and in $\{r, \phi\}$ coordinates. Although the sensor does not monotonically climb the field, it still reaches a neighborhood of constant radius around the maximum point.

V. Conclusions

The paper has described what we call reactive control laws. These are control laws that rely on the interaction between a moving sensor and the sensed measurements that it makes of an unknown environment. With applications to robotic reconnaissance and scanning probe microscopy in mind, we have modeled unknown environments as scalar fields defined on planar domains. The performance of control laws that we have proposed for exploring these unknown fields has been shown to depend on geometric characteristics of the field—specifically certain curvature parameters. Because the curvatures are *a priori* unknown, they are treated as disturbances, and the performance of the control laws has been shown to depend on the magnitude of such disturbances. While the dependence of mobile sensor performance on the geometric characteristics of the unknown field is conceptually attractive, the approach in which unknown geometric parameters are treated as perturbations has the additional advantage that it can be extended to treat sensor noise. It is noted that the controls described above are appropriate for robotic vehicles with enough actuator authority to make kinematic control effective. In most laboratory settings, this is almost always the case. For applications in which dynamic effects need to be accounted for, the designs we have described would need to be further validated and refined.

Previous work ([7], [6]) speaks in some detail about the challenges in designing sensor based feedback control laws for nonholonomic robotic vehicles. While the gradient-climbing and isoline-following controls presented above have been shown to be robust with respect to the given design objectives, it is clear that control gains that are not well matched to the geometric characteristics of the *a priori* unknown fields will result in degraded performance. Research on control laws that adapt to acquired environmental information may provide increased efficiency in the kinds of reconnaissance missions treated here and more broadly in [13]. A further area for future research is sensor based control for exploration of non-stationary fields (such as would occur with diffusing chemical contamination). For such problems, rates of change of the time-varying field will need to be taken into account in controller design, and clearly the motion

primitives we have discussed will need to be modified. The many open problems of this type indicate that the development of new approaches to control for information acquisition has a very rich future.

REFERENCES

[1] *IEEE Transactions on Automatic Control, Special Issue on Networked Control Systems*, 49(9), 2004.

[2] *PROCEEDINGS of the IEEE, Special Issue on Technology of Networked Control Systems*, 95(1), 2007.

[3] *Nature: Taming Complexity*, 473(7346), 2011.

[4] J. Adler. Chemotaxis in bacteria. *Science*, 153(3737):708–716, August 1966.

[5] S.B Andersson and D.Y. Abramovitch. A survey of non-raster scan methods with application to atomic force microscopy. In *Proceedings of the American Controls Conference*, July 2007.

[6] J. Baillieul. The geometry of sensor information utilization in nonlinear feedback control of vehicle formations. In V. Kumar, N.E. Leonard, and A.S. Morse, editors, *Lecture Notes in Control and Information Sciences*, volume 309. Springer-Verlag, 2003.

[7] J. Baillieul and A. Suri. Information patterns and hedging brockett's theorem in controlling vehicle formations. In *Proceedings of the 2003 IEEE Conference on Decision and Control*, pages 556–563, 2003.

[8] J. Baillieul and D. Baronov. Information acquisition in the exploration of random fields. In X. Hu and B. Ghosh, editors, *Three decades of progress in control*. Springer, 2010.

[9] D. Baronov and S.B. Andersson. Controlling a magnetic force microscope to track a magnetized nanosize particle. *IEEE transactions on nanotechnology: Accepted for future publication*, 2009.

[10] D. Baronov and J. Baillieul. Reactvie exploration through following isolines in a potential field. In *Proceedings of the American Control Conference*, pages 2141–2146, 2007.

[11] D. Baronov and J. Baillieul. Autonomous vehicle control for ascending/descending along a potential field with two applications. In *Submited to 2008 American Controls Conference*, 2008.

[12] D. Baronov and J. Baillieul. Search decisions for teams of automata. In *Proceedings of the 47th IEEE Conference on Decision and Control*, pages 1133–1138, 2008.

[13] D. Baronov and J. Baillieul. Decision making for rapid information acquisition in the reconnaissance of random fields. *Proceedings of the IEEE: Special Issue on Interaction Dynamics at the Interface of Humans and Smart Machines*, To appear, 2011.

[14] T. Başar and G. J. Olsder. *Dynamic Noncooperative Game Theory*. Academic Press, London/New York, 1995.

[15] J. Cochran and M. Krstic. Nonholonomic source seeking with tuning of angular velocity. *Automatic Control, IEEE Transactions on*, 54(4):717–731, April 2009.

[16] J. Cochran, A. Siranosian, N. Ghods, and M. Krstic. 3-d source seeking for underactuated vehicles without position measurement. *Robotics, IEEE Transactions on*, 25(1):116–129, February 2009.

[17] J. Cochran and M. Krstic. Source seeking with a nonholonomic unicycle without position measurements and with tuning of angular velocity part i: Stability analysis. In *Proceedings of the 46th IEEE Conference on Decision and Control*, pages 6009–6016, December 2007.

[18] J. Cortes. Distributed gradient ascent of random fields by robotic sensor networks. In *Proceedings of the 46th IEEE Conference on Decision and Control*, pages 3120–3126, December 2007.

[19] A. Dhariwal, G.S. Sukhatme, and A.A. G. Requicha. Bacterium-inspired robots for environmental monitoring. In *Proceedings of the International Conference on Robotics and Automation*, New Orleans, LA, April 2004.

[20] R. Frezza, G. Picci, and S. Soatto. A lagrangian formulation of nonholonomic path following. In *The Confluence of Vision and Control*. Springer Verlag, 1998.

[21] Y.-C. Ho and K.-C. Chu. Team decision theory and information structures in optimal control problems-part i. *IEEE Transactions on Automatic Control*, AC-17(1), 1972.

[22] H.K. Khalil. *Nonlinear Systems*. Prentice Hall, third edition, 2002.

[23] N.E. Leonard, D. Paley, and F. Lekien. Collective motion, sensor networks and ocean sampling. *Proceedings of the IEEE*, 2006.

[24] K. Li and J. Baillieul. Robust quantization for digital finite communication bandwidth control. *IEEE Transactions on Automatic Control*, 49(9):1573–1584, 2004.

[25] Yi Ma, Jana Kosecka, and Shankar S. Sastry. Vision guided navigation for a nonholonomic mobile robot. *IEEE TRANSACTIONS ON ROBOTICS AND AUTOMATION*, 15(3), June 1999.

[26] V. Manikonda, P. S. Krishnaprasad, and J. Hendler. Languages, behaviors, hybrid architechtures and motion control. In John Baillieul and Jan C. Willems, editors, *Mathematical control theory*, pages 200–226. Springer-Verlag New York, Inc., New York, NY, USA, 1998.

[27] Y. Matsumoto. *An introduction to Morse Thoery*. American Mathematical Society, 1997.

[28] C.G. Mayhew, R.G. Sanfelice, and A.R. Teel. Robust source-seeking hybrid controllers for autonomous vehicles. In *2007 American Control Conference, Marriott Marquis Hotel at Times Square, New York City, USA*, 2007.

[29] G.N. Nair and R.J. Evans. Exponential stabilizability of finite-dimensional linear systems with limited data rates. *Automatica*, 29(4):585–593, 2003.

[30] P. Orgen, E. Fiorelli, and N.E. Leonard. Cooperative control of mobile sensor networks: Adaptive gradient climbing in a distributed environment. *IEEE TRANSACTIONS ON AUTOMATIC CONTROL*, 49(8):1292–1302, August 2004.

[31] P. Rigby and S.B. Williams. Adaptive Sensing for Localisation of an Autonomous Underwater Vehicle, in Proceedings of the *Australasian Conference on Robotics and Automation 2005*.
`http://www.araa.asn.au/acra/acra2005/papers/rigby.pdf`

[32] D. J. Struik. *Lectures on Classical Differential Geometry*. Dover, 1988.

[33] S. Tatikonda and S.K. Mitter. Control under communication constraints. *IEEE Transactions on Automatic Control*, 49(7):1056–1068, 2004.

[34] W.S. Wong and R.W. Brockett. Systems with finite communication bandwidth constraints, ii: Stabilization with limited information feedback. *IEEE Transactions on Automatic Control*, 44(5):1049–1053, 1999.

[35] F. Zhang, E. W. Justh, and P. S. Krishnaprasad. Boundary following using gyroscopic control. In *43rd IEEE Conference on Decision and Control, 2004. CDC*, 2004.

[36] Fumin Zhang, Edward Fiorelli, and Naomi Ehrich Leonard. Exploring scalar fields using multiple sensor platforms: Tracking level curves. In *Proceedings of the 46th IEEE Conference on Decision and Control*, pages 3579–3584, December 2007.

[37] F. Zhang and N.E. Leonard. Generating contour plots using multiple sensor platforms. *IEEE Swarm Intelligence Symposium*, 2005.